

Supporting Information

Defective Bismuth-Indium Catalyst Promotes Water Dissociation for Selective Carbon Dioxide Electroreduction to Formate

Jieshu Zhou,^a Liming Li,^{b,c} Hangxing Ren,^{b,d} Haibin Wang,^a Yong Li,^e Kangning Liu,^a Liang Huang,^e Xinyao Yang,^e Zhen Hao,^b Yuguang Zhang,^b Zhichao Wang,^e Xi Wang,^a Jian Ding,^e Yuping Ji,^e Li Wang,^a Hongyan Liang,^{*a}

- a. School of Materials Science and Engineering, Tianjin University, Tianjin 300350, P. R. China
E-mail: hongyan.liang@tju.edu.cn
- b. PERIC Hydrogen Technologies Co., Ltd., Handan 056027, P. R. China
- c. School of Chemical Engineering and Technology, Tianjin University, Tianjin 300072, P.R. China.
- d. School of Materials Science and Engineering, Shanghai Jiao Tong University, Shanghai 200240, P.R. China
- e. CETC Deqing Huaying Electronics Co.,LTD., Deqing, Zhejiang, 313200, P.R. China

Experimental section

Chemicals

Bismuth (III) nitrate pentahydrate ($\text{Bi}(\text{NO}_3)_3 \cdot 5\text{H}_2\text{O}$), potassium bicarbonate (KHCO_3), and potassium borohydride (KBH_4) were purchased from Aladdin. Indium nitrate pentahydrate (III) ($\text{In}(\text{NO}_3)_3 \cdot 5\text{H}_2\text{O}$), sodium hypophosphite (NaH_2PO_2), potassium hydroxide (KOH), and isopropanol (IPA) were purchased from Macklin. Nafion solution (5wt%), dimethyl sulfoxide (DMSO), and deuterium oxide (D_2O) were purchased from Sigma-Aldrich. All chemicals were used directly without further treatment.

Synthesis of Catalysts

Synthesis of BiIn-P pre-catalyst: Deionized (DI) water (18.2 M Ω) was used as solvent for the synthesis. The BiIn-P pre-catalyst was synthesized using a three-neck round-bottomed flask. First, a solution was made by dissolving 0.002 mol of $\text{Bi}(\text{NO}_3)_3 \cdot 5\text{H}_2\text{O}$ and 0.004 mol of $\text{In}(\text{NO}_3)_3 \cdot 5\text{H}_2\text{O}$ in DI water (20 mL) in a three-neck round-bottomed flask with continuous stirring at room temperature. Then, 230 mg NaH_2PO_2 was added to the above solution with continuous oxygen flushing. The oxygen was flushed throughout the whole synthesis process. After 5 min, fresh-made 20 mL of KBH_4 aqueous solution (1.2 M) was added into the above solution with vigorous stirring. After 1 h, the precipitate was collected by centrifuge and washed with DI water and ethanol, followed by vacuum drying at 60 °C overnight.

The synthesis methods of Bi-P pre-catalyst and In-P pre-catalyst are similar to the method for synthesizing BiIn-P pre-catalyst without adding $\text{In}(\text{NO}_3)_3 \cdot 5\text{H}_2\text{O}$ or $\text{Bi}(\text{NO}_3)_3 \cdot 5\text{H}_2\text{O}$ while keeping the total molar concentration as constant.

The synthesis method of BiIn pre-catalyst is similar to the method for synthesizing BiIn-P pre-catalyst without adding NaH_2PO_2 .

Physicochemical characterization

The morphologies of the synthesized catalysts were characterized by field-emission scanning electron microscopy (SEM, Hitachi S-4800), transmission electron microscopy (TEM, JEM-2100F), and energy-dispersive X-ray spectroscopy (EDS). The phase composition and crystallinity of the synthesized catalysts were characterized by powder X-ray diffraction (XRD, Bruker D8) with Cu $K\alpha$ radiation. An X-ray photoelectron spectrometer (XPS, Kratos AXIS SUPRA+) was used to analyze the chemical states of the synthesized catalysts. *In-situ* Raman experiments were performed using a Renishaw spectrometer (Renishaw, inVia microscope) in a homemade CO_2 -saturated 0.1 M KHCO_3 aqueous solution as the electrolyte.

Electrode preparation

To prepare the deposition ink, 10 mg of the precursor was dispersed in a mixture of 0.40 mL IPA, 0.45 mL DI water, and 50 μL 5wt% Nafion solution and then sonicated for at least 1 hour. The ink was air-brushed onto $2 \times 4 \text{ cm}^2$ carbon paper (Toray TGP-H-060 with an MPL layer).

Electrochemical Measurements

The CO_2 electroreduction performance activity of the catalysts was investigated in 1.0 M KOH electrolyte by using a flow-cell configuration connected to an electrochemical workstation (CHI660E). We cut the as-prepared spray-coated gas diffusion layer into $1 \times 1 \text{ cm}^2$ electrodes for testing. Flow-cell configuration consists of catalysts spray-coated gas diffusion layer as the cathode ($1 \times 1 \text{ cm}^2$), an anion exchanged membrane (AEM, Fumasep FAA-3-PK-130) as the membrane, and Ni foam as the anode ($1 \times 1 \text{ cm}^2$), Ag/AgCl was used as the reference electrode. CO_2 gas flowed behind the gas diffusion layer at a rate of 50 mL/min. The gaseous products were detected by GC (GC-2060A) equipped with a thermal conductivity detector (TCD) and flame ionization detector (FID) detector. Liquid products were quantified by analyzing the collected electrolytes using NMR (Bruker, AVANCE IIIITM HD 400 MHz). DMSO was added as an internal standard. All the electrode potentials were converted to values regarding the RHE using the following equation:

$$E_{\text{RHE}} = E_{\text{Ag/AgCl}} + 0.197 \text{ V} + 0.0591 \times \text{pH} + 85\% iR$$

where R is the EIS-determined series resistance. R was measured using the electrochemical impedance spectroscopy technique (EIS, frequency ranges from 100 kHz to 0.1 Hz and amplitude of 5 mV).

The MEA electrolyser was composed of anode and cathode flow field plates with a serpentine-configuration flow field for the continuous supply of anolyte (0.1 M KCO_3) and humidified CO_2 . The MEA was composed of three components: a cathode electrode (catalysts sprayed onto a carbon paper), an anode electrode (iridium oxide deposited titanium foam), and an anion exchange membrane (AEM, Sustainion X37-50 grade 60 membrane). The full-cell potentials are presented without iR -correction.

Theoretical calculation details

All DFT calculations were carried out within the periodic plane wave framework as implemented in Vienna Ab initio Simulation Package.¹ The (003) surface of Bi, the (101) surface of In, and the (310) surface of Bi_3In_5 were used as the models. We use the generalized gradient approximation (GGA) with Perdew-Burke-Ernzerhof (PBE) form to describe the exchange-correlation contributions to the total energy.² Plane-wave cut-off energy of 400 eV and a $3 \times 3 \times 1$ Γ -centered k-points grid generated by

the Monkhorst-Pack scheme were used for all the calculations. The convergence criteria for the electronic self-consistent iteration energy and force were set to 10^{-5} eV and 0.05 eV/Å,

The reaction energies (ΔG) were obtained by:
$$\Delta G = \Delta E_{\text{DFT}} + \Delta \text{ZPE} - T\Delta S$$

Where ΔE_{DFT} is the reaction energy calculated from DFT; ΔZPE is the zero-point energy; ΔS is the change in entropy. In this work, the values of ΔZPE and ΔS of intermediate were obtained by vibration frequency calculation. The following corrections were applied to partially counterbalance the overestimation from DFT calculations: CO_2 (0.45 eV), H_2 (- 0.09 eV), and HCOOH (0.20 eV).³

Supplementary Figures

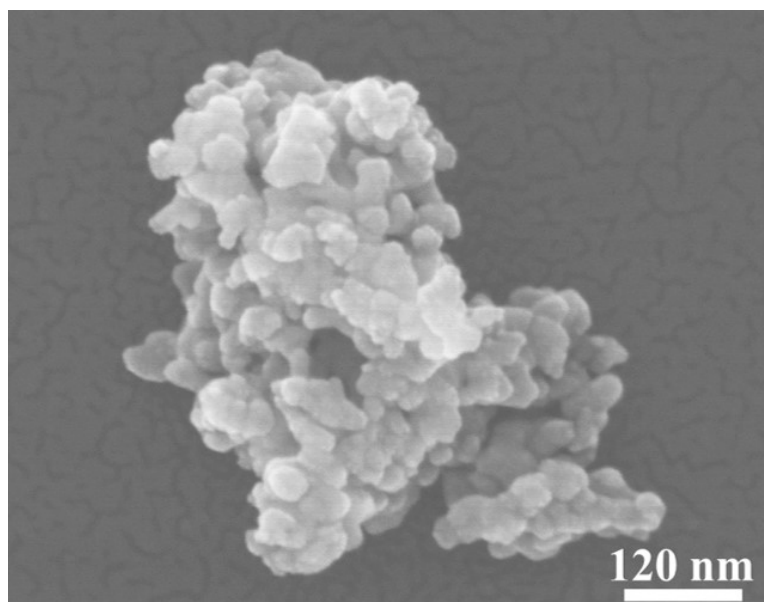


Fig. S1. SEM image of the BiIn-P pre-catalyst.

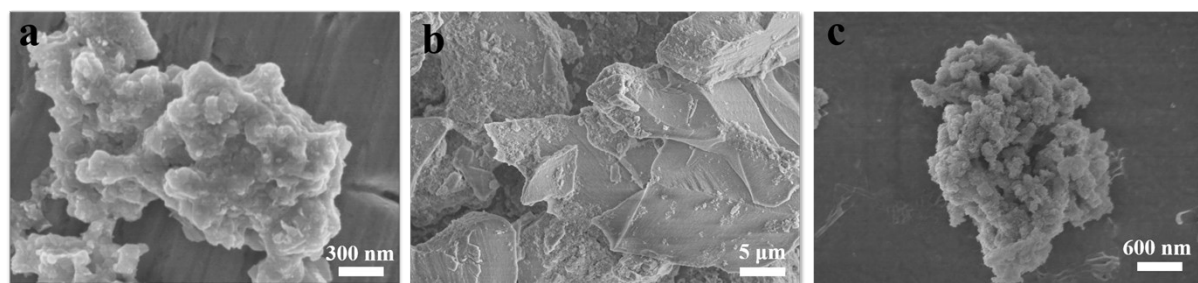


Fig. S2. SEM images of (a) Bi-P, (b) In-P, and (c) BiIn pre-catalysts.

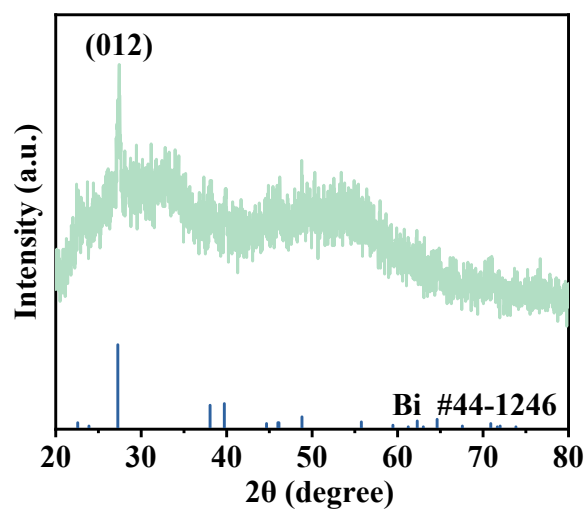


Fig. S3. XRD pattern of the BiIn-P pre-catalyst.

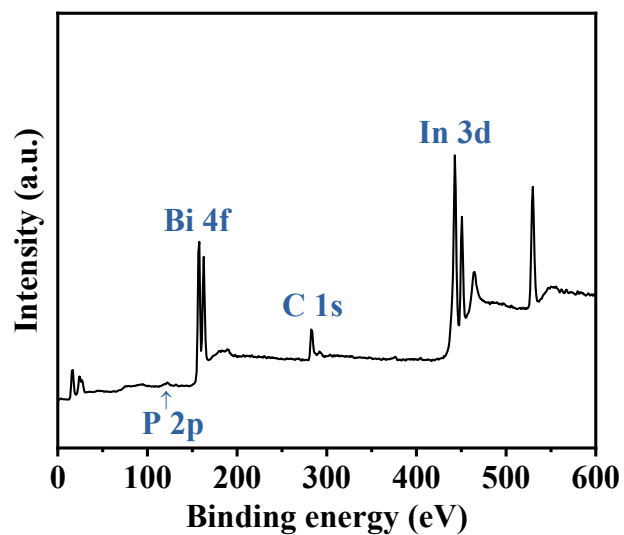


Fig. S4. XPS survey spectrum of the BiIn-P pre-catalyst.

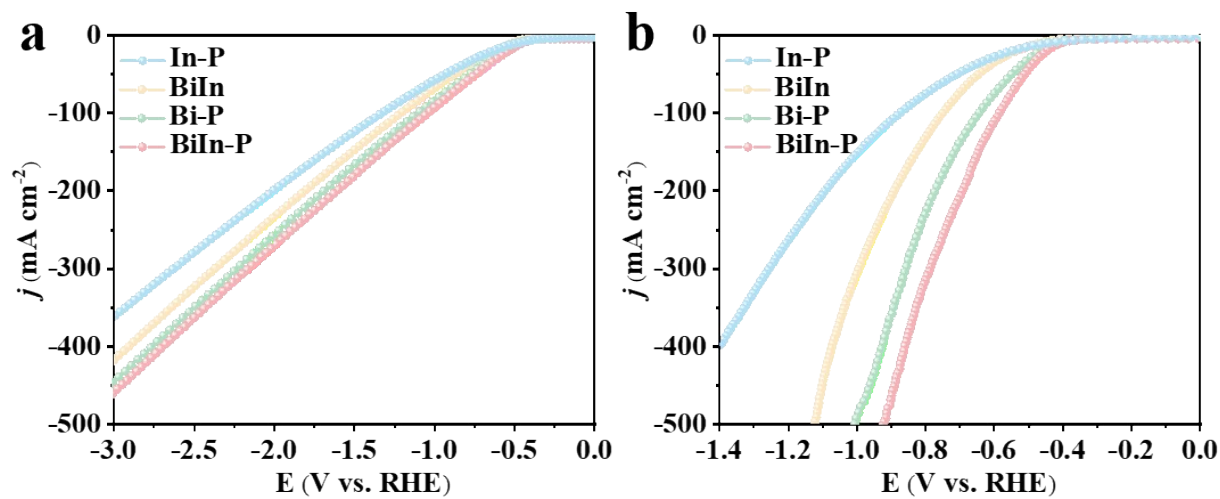


Fig. S5. LSV results of In-P, BiIn, Bi-P, and BiIn-P pre-catalysts in 1.0 M KOH (a) without and (b) with iR compensation.

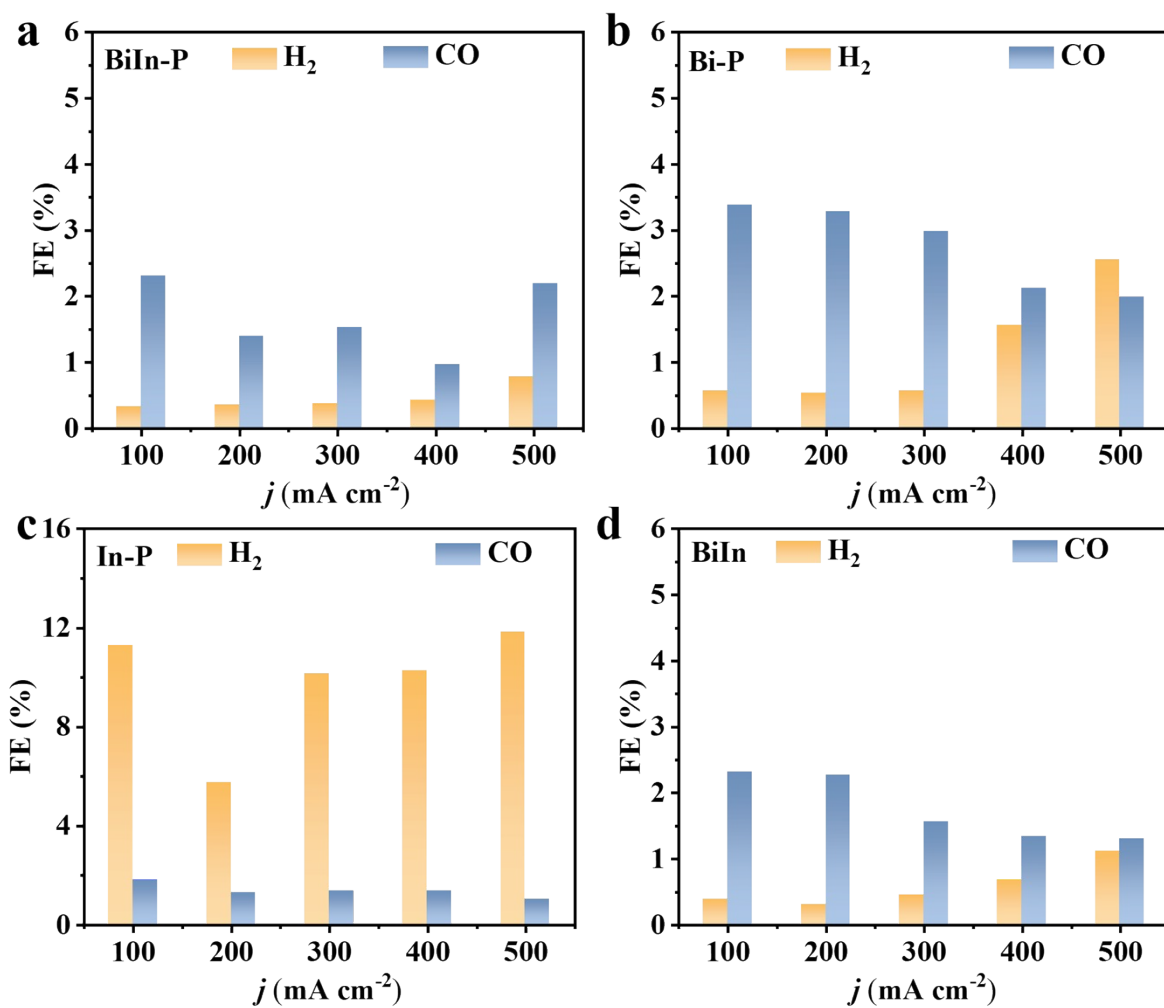


Fig. S6. Faradaic efficiencies of H₂ and CO for (a) BiIn-P, (b) Bi-P, (c) In-P, and (d) BiIn at different current densities in 1.0 M KOH.

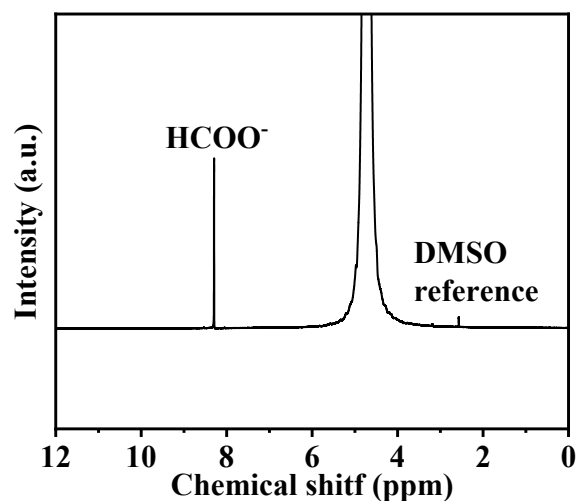


Fig. S7. NMR spectrum of the liquid product in the Flow-cell test.

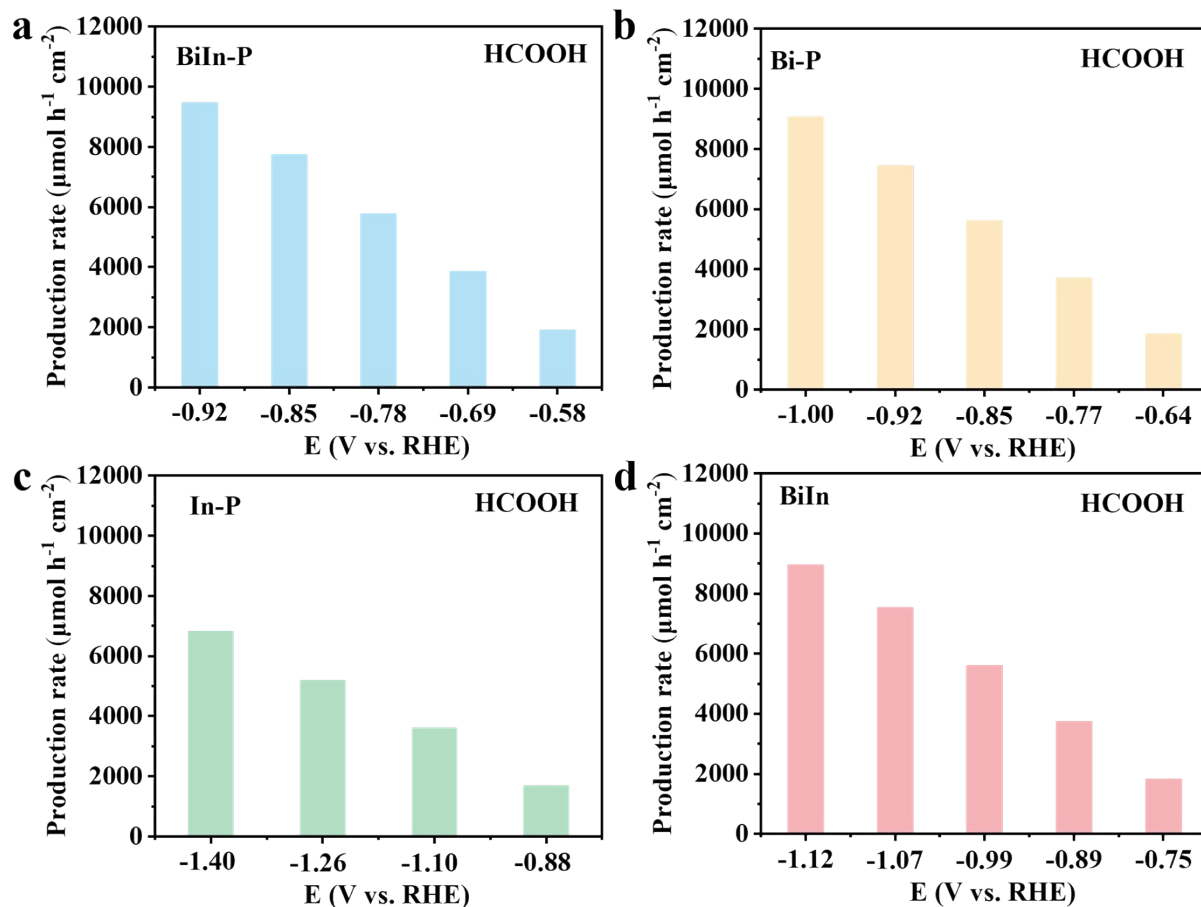


Fig. S8. Production rate of HCOOH over BiIn-P, Bi-P, In-P, and BiIn pre-catalysts at various potentials.

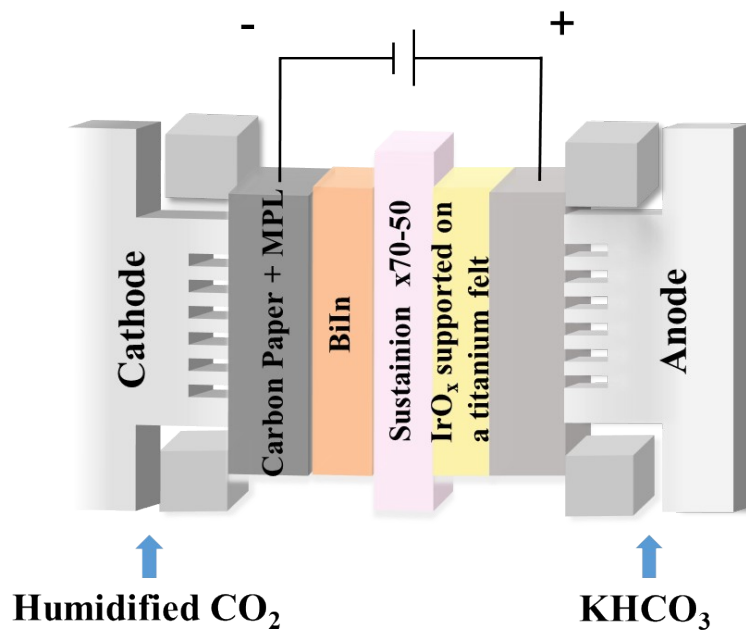


Fig. S9. Schematic diagram of CO₂ reduction in an MEA.

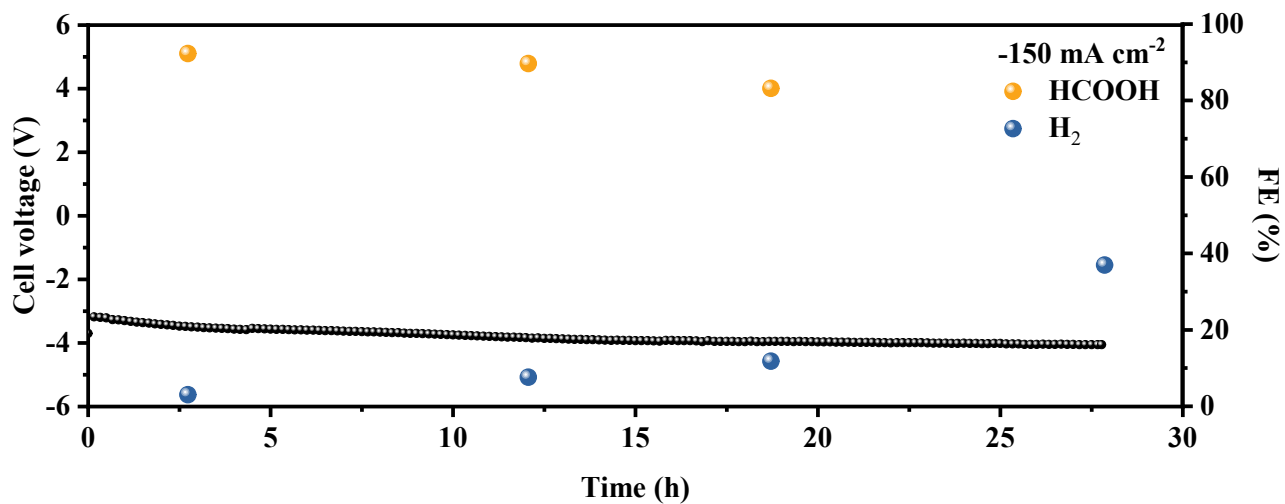


Fig. S10. Long-term chronopotentiometry result and the FEs of H₂ and HCOOH for the BiIn-P pre-catalyst in an MEA.

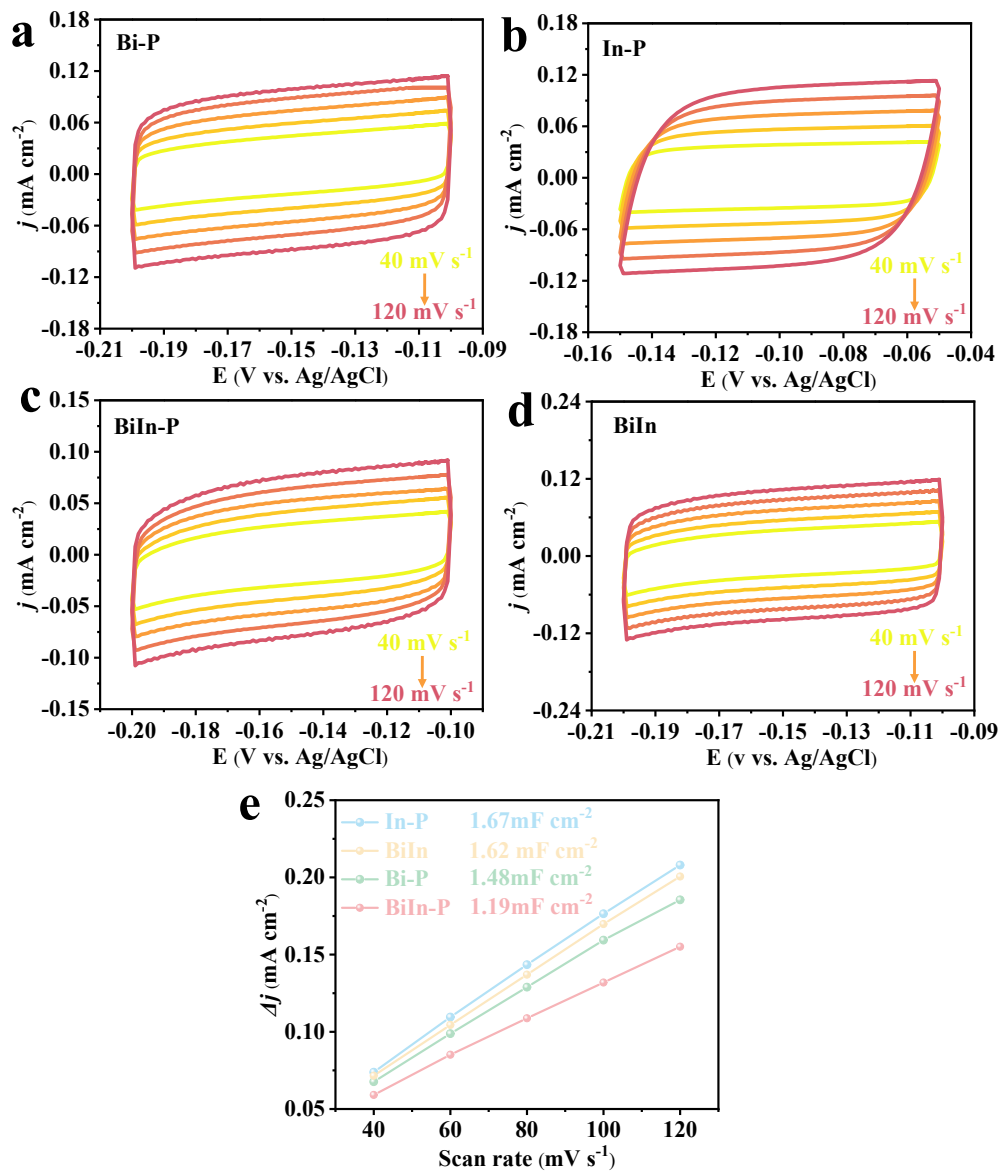


Fig. S11. CV curves of (a) Bi-P, (b) In-P, (c) BiIn-P, and (d) BiIn pre-catalysts in 1.0 M KOH. (e) Differences in current density variation against the scan rate, and using a linear fitting method to estimate the C_{dl} .

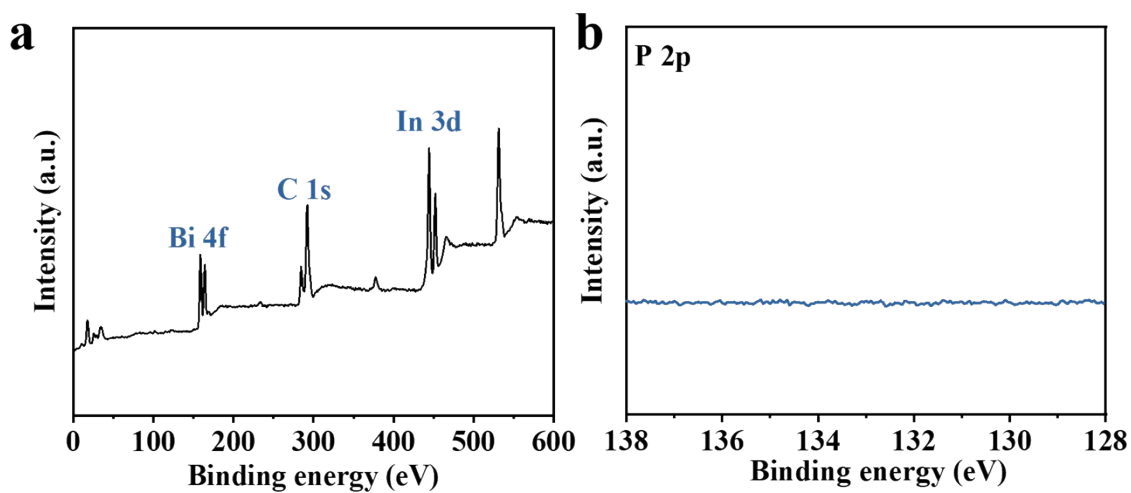


Fig. S14. (a) XPS survey spectra and (b) P 2p XPS spectra of BiIn-P pre-catalysts after the reaction.

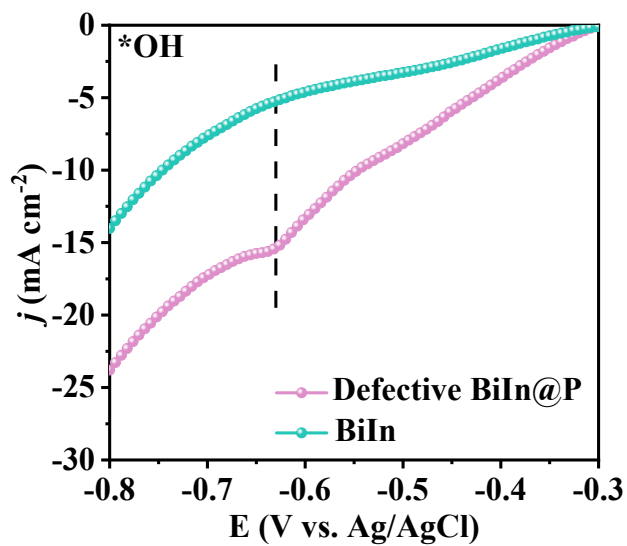


Fig. S15. LSV curves of Defective BiIn@P and BiIn in Ar-saturated 1.0 M KOH.

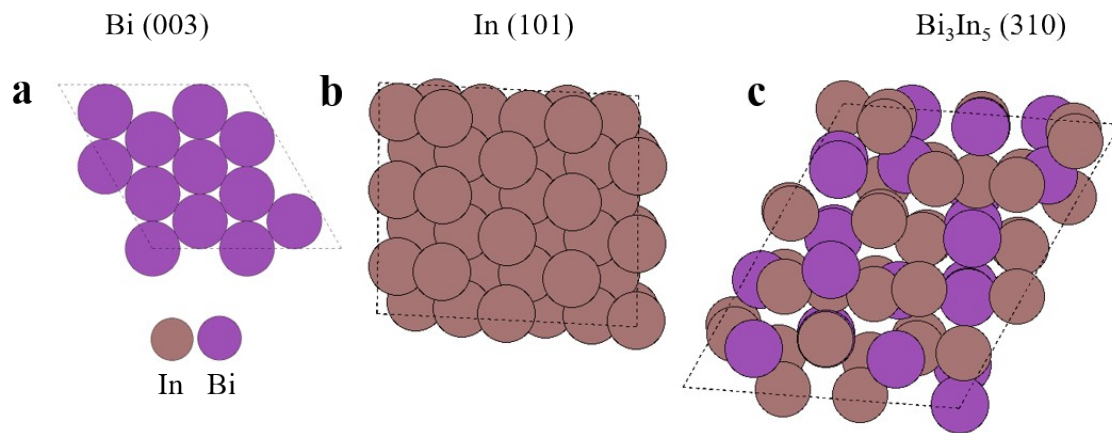


Fig. S16. DFT configurations for Bi (003), In (101), and Bi₃In₅ (310), respectively.

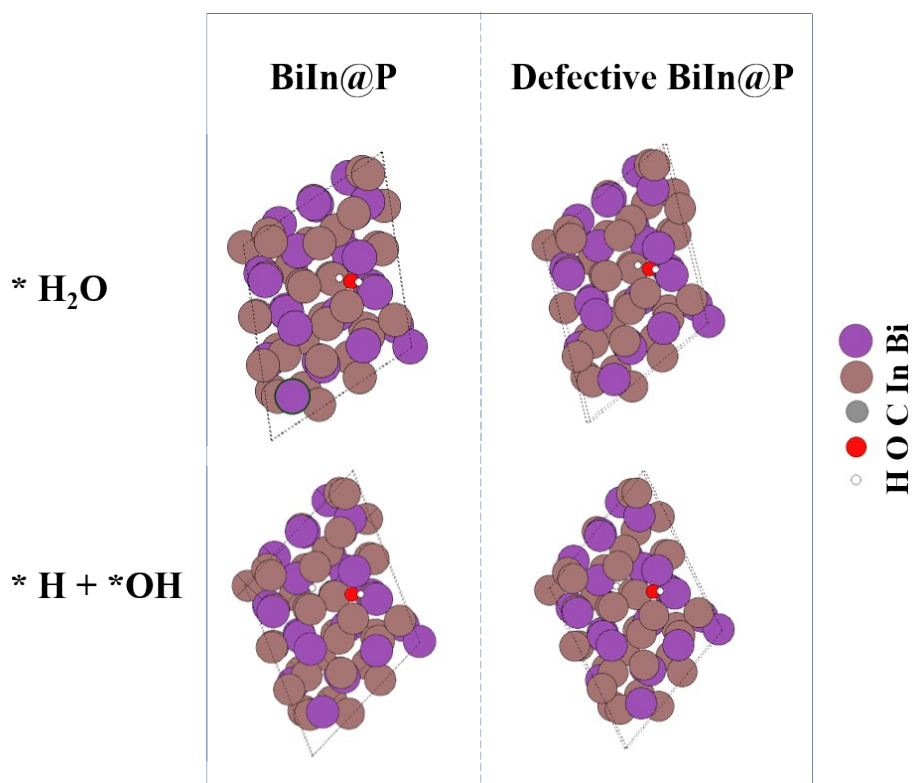


Fig. S17. DFT configurations for $*\text{H}_2\text{O}$ and $*\text{H} + *\text{OH}$ on the BiIn@P and Defective BiIn@P, respectively.

Table S1. Comparison of CO₂ electroreduction performance between Defective BiIn@P and reported catalysts.

Catalyst	Current density	FE _{HCOOH}	Reference
Defective BiIn@P	500 mA cm⁻²	97.3%	This work
SnPc-8F@CNTs	404 mA cm ⁻²	91.7%	<i>Appl. Catal. B: Environ.</i> , 2023, 123650.
Cu ₂ S/1%SnO ₂ @C	15.6 mA cm ⁻²	88%	<i>J. Colloid Interface Sci.</i> , 2024, 655 , 909-919.
BiOBr(BOB)	148 mA cm ⁻²	91%	<i>Nat. Catal.</i> , 2023, 6 , 796-806.
S3-Cu ₂ O-70	100 mA cm ⁻² 400 mA cm ⁻²	75% 65%	<i>Adv. Funct. Mater.</i> , 2023, 33 , 2213145.
SnS ₂ @SnO ₂	200 mA cm ⁻²	92.2%	<i>ACS Appl. Mater. Interfaces</i> , 2023, 15 , 7529-7537.
PbCO ₃ @CNS	9.65 mA cm ⁻²	98.15%	<i>Appl. Catal. B: Environ.</i> , 2023, 326, 122404.
PdCuAuAgBiIn	200 mA cm ⁻²	87%	<i>Adv. Mater.</i> , 2023, 35 , 2209242.
In/In ₂ O ₃ -1600	140 mA cm ⁻²	94%	<i>Adv. Funct. Mater.</i> , 2023, 33 , 2209114.
BiOI	94 mA cm ⁻²	90%	<i>J. Mater. Chem. A.</i> , 2022, 10 , 1309-1319.
Bismuthene nanoflakes	10.5 mA cm ⁻²	96.3%	<i>Nano Lett.</i> , 2023, 23 , 10512–10521.
BH-10	444.1 mA cm ⁻²	95.7%	<i>Angew. Chem. Int. Ed.</i> , 2023, 62 , e202313522.
Ti-Bi NSs	224 mA cm ⁻²	96.3%	<i>Small</i> , 2023, 19 , 2302253.

BiNN-CFs	over 400 mA cm ⁻²	95.7%	<i>Adv. Energy Mater.</i> , 2022, 12 , 2103960.
Bi ₅ Sn ₆₀	34 mA cm ⁻²	94.8%	<i>Chem. Eng. J.</i> , 2022, 428 , 130901.
S-Bi-NSs	over 300 mA cm ⁻²	~98%	<i>ACS Appl. Mater. Interfaces.</i> , 2021, 13 , 20589–20597
Bi ₅ In ₅ nanofibers	~225 mA cm ⁻²	96.8%	<i>J. Mater. Chem. A</i> , 2023, 11 , 11445-11453.
BiIn ₅ -500@C	~8 mA cm ⁻²	97.5%	<i>J. Colloid Interface Sci.</i> , 2022, 612 , 235-245.
BiIn alloy NPs	250 mA cm ⁻²	97.8%	<i>Appl. Catal. B: Environ.</i> , 2023, 311, 121377.

References

- 1 G. Kresse, J. Hafner, Ab initio molecular-dynamics simulation of the liquid-metal--amorphous-semiconductor transition in germanium, *Phys. Rev. B*, 1994, **49**, 14251-14269.
- 2 G. Kresse, J. Furthmüller, Efficient iterative schemes for ab initio total-energy calculations using a plane-wave basis set, *Phys. Rev. B*, 1996, **54**, 11169-11186.
- 3 L. Li, A. Ozden, S. Guo, F.P. Garci, A. de Arquer, C. Wang, M. Zhang, J. Zhang, H. Jiang, W. Wang, H. Dong, D. Sinton, E.H. Sargent, M. Zhong, Stable, active CO₂ reduction to formate via redox-modulated stabilization of active sites, *Nat. Commun.* 2021, **12**, 5223.